한국해양공학회지 제21권 제6호, pp 16-25, 2007년 12월 (ISSN 1225-0767)

Diagonal Tension Failure Model for RC Slender Beams without Shear Reinforcement Based on Kinematical Conditions (II) - Verification

YOUNG-MIN YOU* AND WON-HO KANG**

*Dept. of Civil, Architectural and Environmental Engineering, University of Missouri-Rolla (UMR), USA
**Dept. of Civil and Ocean Engineering, Dong-A University, Busan, Korea

KEY WORDS: RC Slender beam test, Shear span ration, Splitting failure

ABSTRACT: *In a companion paper, a rational mechanical model to predict the entire behavior of point-loaded RC slender beams (a/d > 2.5) without shear reinforcement was developed. This paper presents the test results of 9 slender shear beams and compares them with analytical results performed by the proposed model. They are grouped by two parameters, which are shear span ratio and concrete strength. Three kinds of concrete strength the 26.5, 39.2, and 58.8 MPa were included as a major experimental parameter together with different shear span ratios ranging from 3 to 6 depending on the test series. Tests were set up as a traditional 3 point bending test. Various measurements were taken to monitor abrupt shear failure. Test results were not only compared with analytical results from the proposed model, but also other formulas, to consider the various aspects of shear failure such as kinematical conditions or shear capacity. Finally, a review of the proposed model is presented with respect to the shear transfer mechanisms and the effect of test parameters. Results show that several assumptions and proposals adopted in the proposed model are rational and reasonable.*

1. Introduction

Shear capacity of RC slender beams without shear reinforcement depends on a number of influence parameters, which are strength of concrete, longitudinal reinforcing ratio, shape or size of longitudinal reinforcement, shear span-to-depth ratio, axial force or amount of prestress, and depth of the members which account for size effect. Based on experimental results, the following major shear transfer mechanism has been identified. (a) Shear stresses in the uncracked compression zone of concrete; (b) Inclined compression force in the compression zone corresponding to arch action; (c) Interface shear transfer along the diagonal tension crack through aggregated interlock; (d) Residual normal stresses across the diagonal tension crack due to strain softening; (e) Dowel action of the longitudinal reinforcement.

The contribution of concrete for shear capacity (the first four components) has been investigated by many experimental studies, and proved that it is responsible for most of shear force. As a result, the contribution of dowel action by longitudinal reinforcement used to be ignored in early investigations. However, it was shown by Chana that the longitudinal reinforcement played a main role to control the shear failure mechanism. Because it prevents a diagonal tension crack from opening, shear mechanisms affected by this prevention such as aggregate interlock or strain softening are strongly controlled by longitudinal reinforcement. In addition, the longitudinal reinforcement controls the propagation of the diagonal tension crack into the compressive zone, which causes a reduction of uncracked concrete area carrying shear. Chana used high-speed photography and continuously recorded crack widths at critical locations to investigate the history of the mechanisms occurring in the flexural-shear failure. Chana showed that the first crack opened in an unstable manner is associated with the horizontal crack of concrete at the level of the longitudinal reinforcement. This is closely followed by further opening and extension of the pre-existing diagonal shear crack, resulting in the failure of the concrete compression zone under a combination of compression and shear stresses. It was concluded that the compression zone is intact at the onset of failure, and that the flexural-shear failure is triggered by horizontal crack along the longitudinal reinforcement.

Even the most researchers agree that the horizontal crack works as an agency of failure, there are still controversies about the cause of horizontal crack. Some researchers advocate that the cause is dependent on bonding failure, the others do the cause is dependent on the splitting failure induced by dowel action. In addition, there are other controversies about the forming time of horizontal crack. That could be before or after the ultimate loading state.

To account for bonding failure, test beams having a small number of thick steel reinforcement and a large number of

교신저자 유영민 : 부산광역시 사하구 하단2동 840번지
051-200-5744 ymy4297@nate.com

thin steel reinforcement with same reinforcement ratio were compared with each other by Leonhardt and Walther (1962). As a result, shear strength of beams having a small number of thick steel reinforcement is lower than contraries. This phenomenon is considered as a fundamental basis of bonding failure. But, this phenomenon can be also a basis for opposers. According to Bhal (1968), relations between shear strength and steel circumference was not strictly affected to each other. The statistical result from shear database showed that the correlation coefficient between shear strength and steel circumference/area (u_s/A_s) was only 0.07. Another interesting results can be found in test by Ahmad et al. (1986). A horizontal crack developed in different manners depending on reinforcement ratios. When reinforcement ratio was high, horizontal crack developed into primary and secondary cracks. Otherwise, when reinforcement ratio was low, horizontal crack developed almost parallel to longitudinal reinforcement.

From reviewing former researches, proper test parameters were selected to verify the efficiency of the proposed model. Test was carried out with respect to the representative parameters and compared with the analytical results by the proposed model in various aspects like kinematical conditions and shear transfer mechanisms.

2. Test Program

To validate the assumptions of the proposed model in this research, the failure test of RC slender beams without shear reinforcement was carried out. Although there are many good test results for RC slender beams, it is not easy to get an available data about when the horizontal crack starts and the failure begins. It is very difficult to measure or inspect shear failure behavior accurately, because shear failure of RC slender beams without shear reinforcement is abrupt in most case. Therefore, in some cases, same test specimens were tested with different measuring or loading methods to get better test results.

2.1 Test specimens and materials

Depending on major parameter, concrete strength, test series are divided into three. The reason taking concrete strength as a major parameter is related to shear transfer mechanisms. Because, they are mainly affected by concrete strength as mentioned above. With the secondary parameter, shear span ratios, test series are divided into four. The reason taking it as the secondary parameter is related with the geometrical assumption of proposed model. They are summarized in Table 1. Although other parameters like reinforcing ratio and size effect are not treated in this paper, it is possible to prove the efficiency of proposed model with these test series. Because, the most important issue on the proposed model is investigating the participation of shear transfer mechanisms depending on kinematical conditions based on assumed geometrical shape of diagonal tension failure. Test specimens were cast in pairs in wooden moulds and were partly wet cured for four weeks before being taken into the laboratory for instrumentation and testing. Details of the test beams and rig are shown in Table 2 and Fig. 1. The mix proportion of concrete is also shown in Table 3. Concrete and steel strength is averaged characteristics.

Table 1 Properties of test specimens

Series	ID	*fck* (MPa)	*a/d*	*d* (mm)	*b* (mm)	ρ	Steel
I	I-3	26.5	3	250	250	0.0179	3@D22
	I-4	〃	4	〃	〃	〃	〃
	I-5	〃	5	〃	〃	〃	〃
	I-6	〃	6	〃	〃	〃	〃
II	II-S1	39.2	4	〃	〃	〃	〃
	II-S2	〃	〃	〃	〃	〃	〃
	II-S3	〃	〃	〃	〃	〃	〃
III	III-S1	58.8	〃	〃	〃	〃	〃
	III-S2	〃	〃	〃	〃	〃	〃

Table 2 Strength of materials

Series	$f_{c,28}$ (MPa)	f_y (MPa)
I	29.4	490
II	41.7	520
III	55.5	421

Table 3 Mix properties of concrete

Series	*fck* (MPa)	*dmax* (mm)	Air (%)	*W/C* (%)	*S/A* (%)	*Adm.* (kg/m^3)	Fly ash (kg/m^3)
I	26.5	25	4.5±1.5	43	40		
II	39.2	25	4.5±1.5	34.3	36	-	-
III	58.8	19	4.5±1.5	30	37.8	13.5	50

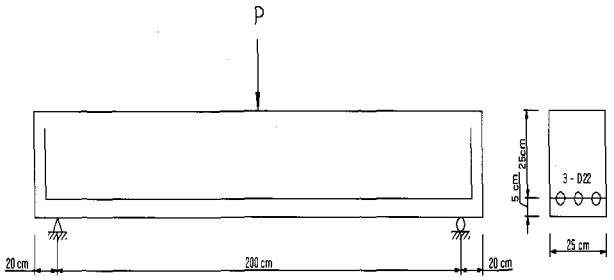

Fig. 1 Details of test specimen

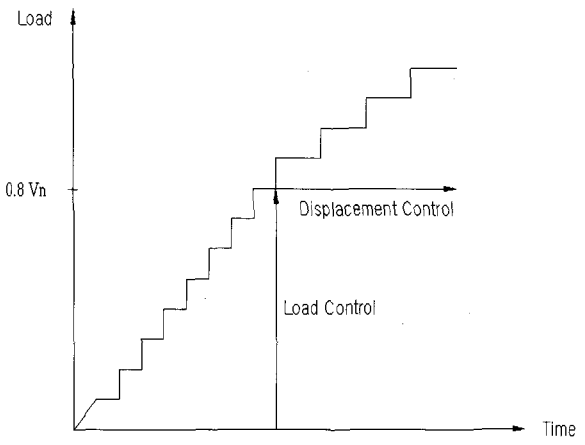

Fig. 2 Test control process

2.2 Test procedure

The beams were subjected to three-point bending test, as illustrated Fig. 1, which shows the test setup prior to testing. An automatic data acquisition system was used to monitor loadings, as well as deflections and deformations in the concrete and reinforcement. The load was applied to the beam step by step with load control before part of nominal strength, $0.8V_n$, and with displacement control after load control state by means of hydraulic actuators and was measured with a load cell, as illustrated Fig. 2. At the end of each step, cracks were sketched and measurements of deflections and strain gage readings were recorded for later processing. Only one specimen, II-D1, is loaded one cycles's unloading and reloading procedure to see the effect of less aggregate interlock

2.3 Measuring method

According to the goal of test beams, different measurements given in Table 4 were carried out.

Table 4 Measurements for test specimens (U: upper, L: lower)

Series	ID	LVDT		Steel gage		Omega age	
		U	L	U	L	U	L
I	I-3	7@15	9@15	-	-	11@15	11@15
	I-4	7@20	9@20	-	-	11@20	11@20
	I-5	7@25	9@25	-	-	11@25	11@25
	I-6	6@30	7@30	-	-	9@30	9@30
II	II-S1	-	7@25	10@20	5@20	3@30	3@30
	II-S2	-	〃	〃	〃	6@30	6@30
	II-D1	-	〃	〃	〃	-	-
III	III-S1	4@40	5@40	〃	5@40	3@30	7@30
	III-S2	4@40	5@40	〃	〃	〃	〃

2.3.1 Test series I

This series is mainly focused on verifying the efficiency of assumed failure shape. Same measuring methods are given to this series with varying LVDTs at spacing $L/10$ to upper and lower part. and omega gages having same spacing with LVDTs.

2.3.2 Test series II

Because series II take roles of standard for slenderness, more detailed measurements are given to this series. They have same measuring apparatus like Demec gages measuring whole surfaces's mean strain value, and LVDTs spaced by 25 cm each other. Besides them, by means of different measuring methods, the local and overall behavior of shear failure has been investigated in detail.

2.3.3 Test series III

This series has same measurements, which are as follows ; LVDTs spacing 40 cm in upper and lower part, steel gages spacing 20 cm in lower part and spacing 40 cm in upper part, three omega gages spacing 30 cm in upper part and seven omega gages spacing 30 cm in lower part.

3. Test Results and Discussion

3.1 Failure pattern and ultimate strength

Depending on the series or the parameters, failure patterns were different. Two beams of test series III failed more brittle than other beams. In this test series, it was difficult to predict the shear failure strength, or formation of web

diagonal tension crack. However, failure mechanism was apparent. All of them failed abruptly with the horizontal crack along longitudinal reinforcement. They had a similar ultimate strength. III-S1 failed at 186.2 kN, and III-S2 failed at 174.7 kN.

Whereas in test series II, in some cases, the formation of web diagonal tension crack were detected. Especially, beam II -D1 having a different loading condition, which was one cycle loading, showed a little ductile behavior, so a formation of web diagonal tension crack was found. Despite of same properties, series II showed different failure behavior. Although all of them also had a horizontal crack, the location of that was different. II-D1 's horizontal crack reaches to the support of beam and has several macrocracks. Whereas, in II-S1 beam, it is ambiguous to define which one is a main crack, due to many microcracks. Of course this beam also has a smaller splitting crack than II-D1 's one. II- S2 beam showed most apparent failure modes. It has a large splitting crack and several macrocracks. They had also a similar ultimate strength. II-D1 failed at 184.24 kN, and II- S1 failed at 176.1 kN, finally II- S2 failed at 168.76 kN.

In test series I, depending on the shear span ratio, several features were shown. The more shear span ratio increases, the more numbers of flexural cracks increases and behave ductile. Beam I- 6 behaves ductilely until ultimate load, whereas other beams did not. But, most particular point of this series is the location of horizontal crack. Except I- 3, they have a similar location considering the shear span ratio. This can be a proof for proposed model. They also have similar strengths. I- 3 failed at 141.12 kN, I- 4 failed at 143.4 kN, I- 5 failed at 151.3 kN. and I- 6 failed at 146.41 kN. The results are summarized in Table 5.

3.2 Load - deflection relations

Figure 3 and 4 show a representative load-displacement distribution curves along span. As shown in figs, they behave elastically at early load state and have almost symmetrical shape. But, as load increase, they showed unsymmetrical shape and after some load state, parts of the deflections are decreased. It might be caused by the shear rotation, the rotation of the crack tip of diagonal tension crack. For most of test beams, the measurement near collapse is impossible or inaccurate, since the failure is very abrupt. However, some of the measurements show that just before failure a remarkable redistribution takes place.

Figure 5 shows a representative load-displacement curve of mid-span. The curves of test series I show in increasing failure displacement of the series according to shear-span ratio. The beam I-6, with a/d = 6, the curve looks like a typical flexural failure curve. For test series II, the curves just before ultimate load are similar but thereafter the falling branches show differences, which is very sensitive to the loading procedure and apparatus. For test series III, it is impossible to measure the behavior near to failure because of their abruptness.

Table 5 Ultimate shear capacity

ID	Series I				Series II			Series III	
	3	4	5	6	D1	S1	S2	S1	S2
V_{ult}	70.6	71.7	75.7	73.2	92.1	91.1	84.4	93.1	87.4

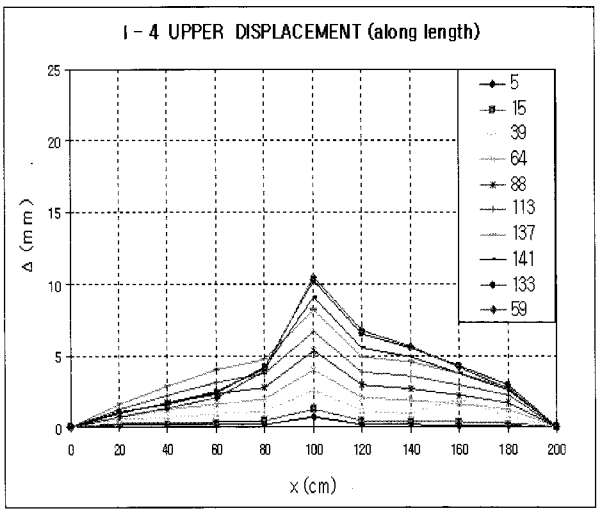

Fig. 3 I-4 Load-upper displacement curve (along length)

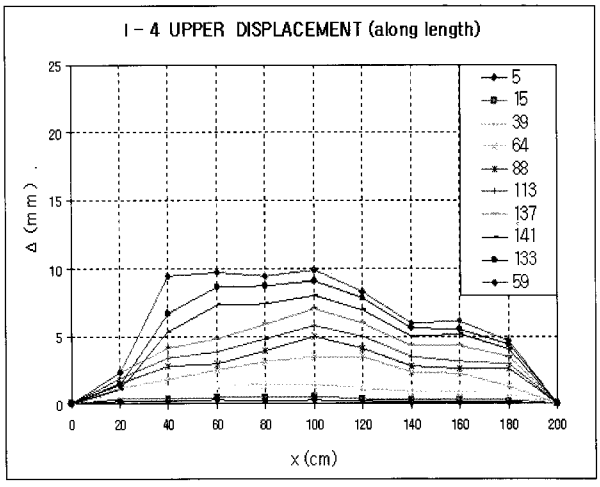

Fig. 4 I-4 Load-lower displacement curve (along length)

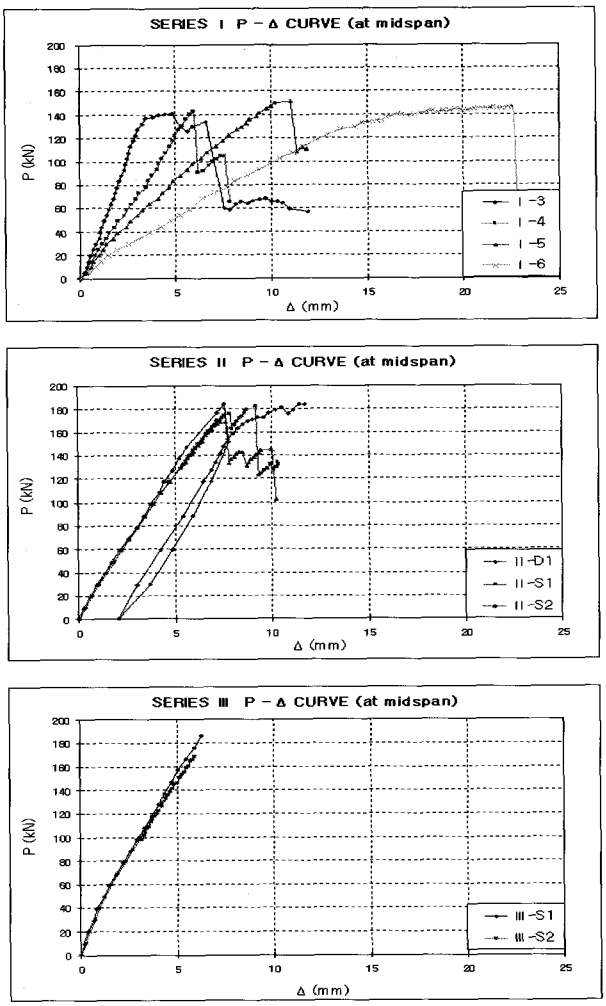

Fig. 5 Load-deflection curves

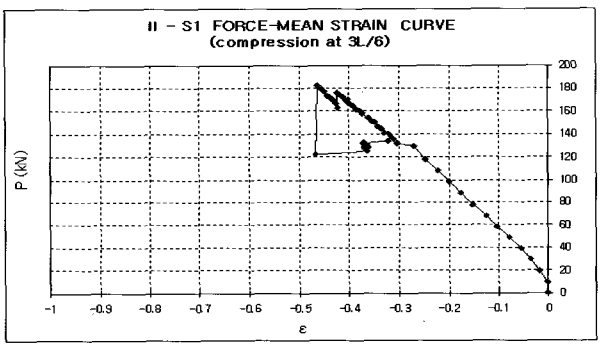

Fig. 6 II- S1 load-mean compressive strain at $3L/6$

3.3 Load-mean strain relations

Because there are too many data in this measurement, representative curves are presented. Figure 6 shows a load-mean strain curves measured by demec gages and omega gage. At the limit state, the mean strain become very sensitive.

4. Verification of Proposed Model

4.1 Shape and initiation point of the diagonal tension crack which Induce failure

To verify the efficiency of assumed failure shape induced by diagonal tension crack, it was compared with the real crack shape of experiment. They are as shown in Fig. 7. Generally it cannot be said that they have good agreement. Test I series showed a better accordance than other series. Especially, beams of Test III showed a bad accordance. There seems to be some tendencies depending on more parameters we considered.

Depending on shear span ratios, the initial point of diagonal tension crack was different. In test beam I -3, cross point occurred over the proposed model. Except test beam I -3, beams of series I show that cross points occurred at a similar location. Depending on concrete strength, inclination of diagonal tension crack was different. As concrete strength decreases, diagonal tension crack developed more steeply. It seems to be responsible to the capacity of forming a rotation hinge at the crack tip. Although the proposal of the initication position equation proposed by Fisher, which is based on 105 test data, it does not includes concrete compressive strength term, and it itself has large variation, some more modification is needed. According to the test results, the efficiency of geometrical assumption can be agreed when it is applied to the shear slender beams.

4.2 Kinematical conditions

Crack sliding and crack width at the crossing point are important, because they are a necessary and sufficient condition for splitting failure of concrete cover. To prove the efficiency of proposed model, crack sliding and width at the crossing point must be compared with test results. Whereas crack width can be measured directly with measuring equipments, it is difficult to measure crack sliding directly with measuring equipments. So, crack sliding can be calculated by using the difference between the upper and lower curvature at the crossing point. This differences also can be verified by comparing strain distributions or neutral axis. After splitting failure, they are also compared with analytical results. Finally moment-mean curvature relations and load-deflection relations are also derived with combining flexural behavior and shear behavior. Because, all of the beams in tests are designed almost with the maximum steel ratio, in estimating their deflections, they showed a very brittle characteristics.

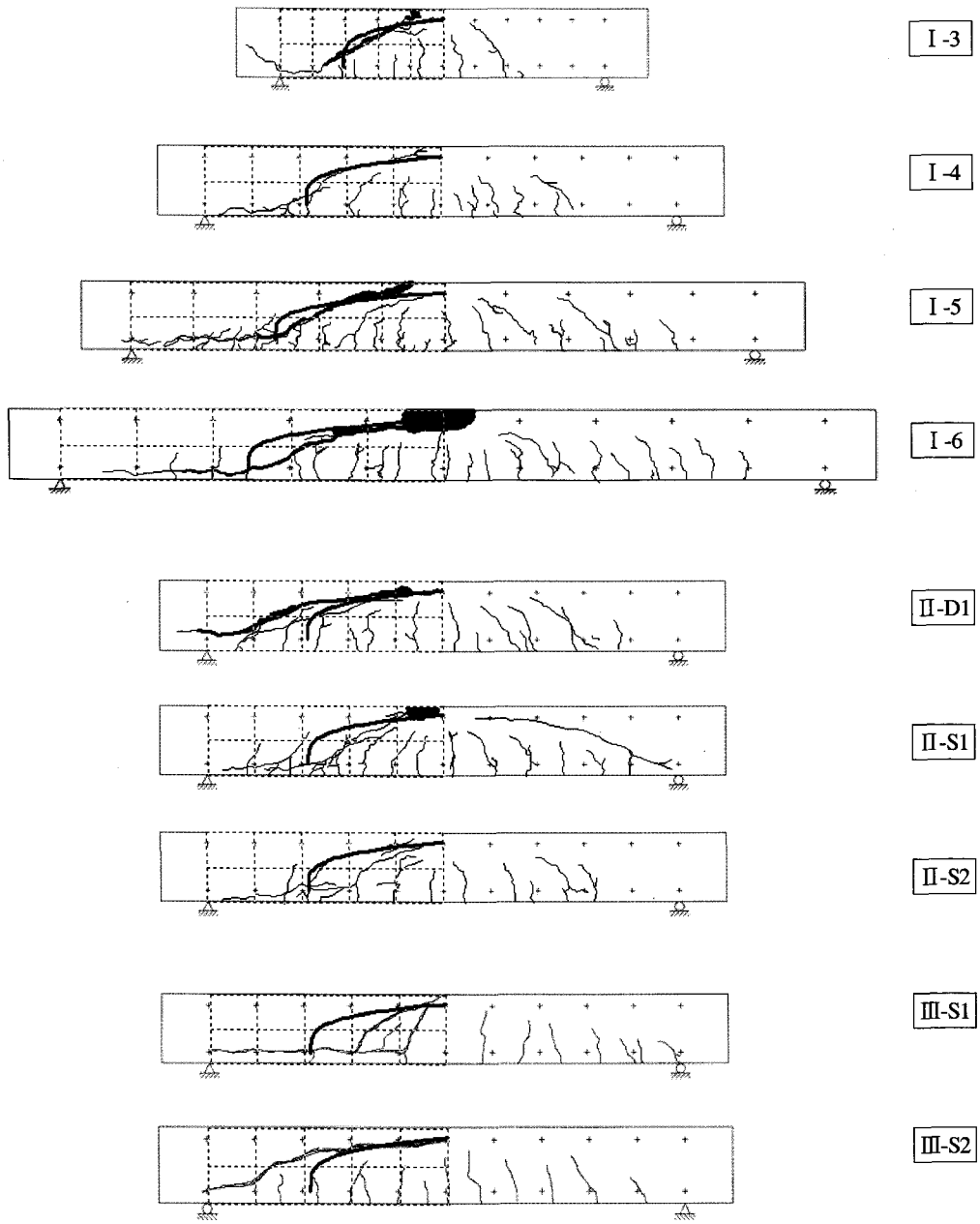

Fig. 7 Comparison of crack patterns between test and analytical result

4.2.1 Comparison of load-mean strain relation

This relation can accounts for the flexural behavior as well as the shear behavior before and after the formation of diagonal tension crack. From the compressive and tensile strains at the mid-span, it is possible to know when rotation angle at the crack tip occur. Sectional strains at the mid-span and crossing point give us a valuable piece of information about the stress trajectories. Figure 8 is a Load-mean strain curve for Series II.

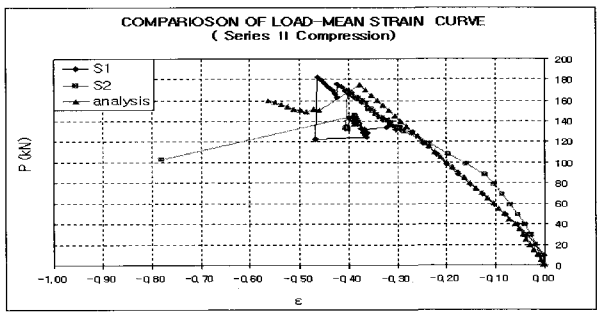

Fig. 8 Comparison of compressive strain (Series II)

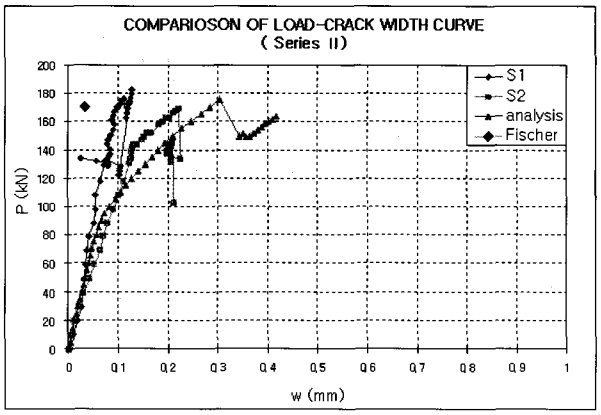

Fig. 9 Comparison of crack width at x_s (Series II)

Table 6 Comparison of crack opening and sliding between test and analysis

Beam	Crack opening			Crack sliding		
	Test	Model	Test/ model	Test	Model	Test/ model
I - 3	0.117	0.315	0.37	0.110	0.099	1.11
I - 4	0.39	0.418	0.93	0.100	0.100	1.00
I - 5	0.390	0.543	0.72	0.150	0.099	1.51
I - 6	0.244	0.690	0.35	0.130	0.099	1.32
II- S1	0.13	0.417	0.31	0.100	0.105	0.95
II- S2	0.211	0.417	0.51	0.080	0.105	0.76
III - S1	0.35	0.404	0.87	0.225	0.110	2.05
III - S2	0.399	0.404	0.99	0.075	0.110	0.68

4.2.2 Crack widths and sliding related to diagonal tension crack

It seems almost impossible to predict either an accurate initial location of diagonal tension crack and the time when shear failure occurs in real beam tests. Although, various measuring systems were adopted in our test, we can only obtain the mean values of crack at the some points, which are the crossing points with measuring equipments. Whereas mean crack widths can be directly measured, crack sliding is more dependent on other measurements like curvature derived from deflections or strain distributions. These values are compared with the results by proposed model at the same locations in real tests. A representative Load-crack width curve at the initial point of diagonal tension crack is shown in Fig. 9.

Although the assumed point in analysis is somewhat different from real experimental one, it can be overcome by concept of mean value, unless a real diagonal crack forms over a proposed diagonal crack. Since proposed model adopts the mean strains, crack spacings and curvatures, diagonal crack widths and sliding have also mean values. Table 6 shows crack width and sliding at the crossing point of diagonal tension crack when shear failure occurs.

4.3 Load-deflection relations

Most members are failed by shear failure abruptly. This features can be detected by moment-curvature or load deflection curves. Fig. 10 is an sectional moment-curvature applied in proposed model. In this relation, CDZ model was adopted. Without shear failure, the ultimate flexural load reaches 1.5 times by ultimate load of shear failure approximately in all beams. In spite of excessive increase of rotation after shear failure, compressive strains of concrete did not reach to a peak value due to dowel splitting. The concepts of mean curvature were adopted with given sectional moment-curvature relation. Curvatures including shear rotation of all members at the mid-span are given in Fig. 11. From these moment-curvature relationships, load-deflection curves were made. A representative curve is shown in Fig. 12.

4.4 Shear transfer mechanisms

From the results of analysis, we can get an information about the participation of shear transfer mechanisms. Several proposals were given in this paper to derive the shear participation of each forces. It was indirectly verified by comparing with kinematical conditions between test and analysis. Most important failure triggering force is a dowel force causing concrete cover splitting, which is a necessary and sufficient condition for shear failure initiation, while the amount of dowel force is not so great. So, it is necessary to know how dowel force acting in concrete cover. It can be explained by satisfying a equilibrium condition of this region. After concrete splitting, all forces acting on diagonal tension crack are discussed.

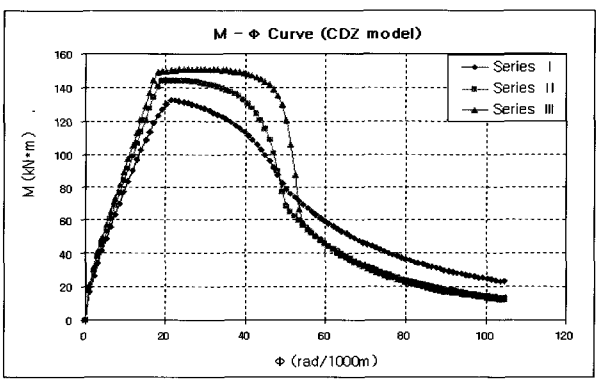

Fig. 10 Sectional moment-curvature diagram

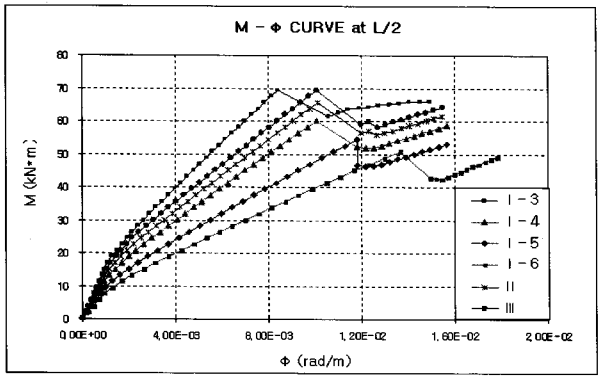

Fig. 11 Moment-curvature relations at $L/2$

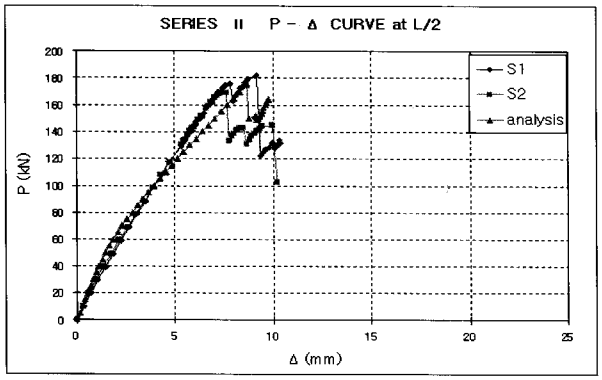

Fig. 12 Load-deflection curve at $L/2$ (Series II)

4.4.1 Splitting failure by dowel force

Timoshenko's equation, which is based on linear elastic principles, does not account for the nonlinear behavior. When concrete cover are splitted, the bearing stresses of concrete under the bar behaves nonlinearly. So, it is necessary to modify the elastic foundation factor, k, associated with nonlinear stress-strain relationship. This value makes concrete cover failed gradually. Figure 13 shows the distance of the zero deflection. This distance is a boundary condition for equilibrium. Figure 14 shows increase of bearing stresses under the bar with splitting failure capacity.

4.4.2 Participation of shear capacity

Proposed model makes it possible to derive the participation of shear capacity before and after shear failure. Because all transfer forces are affected by experimental parameters, the proposed model has an important merit. Figure 15 shows participation of shear capacity of all members at the time of shear failure. From this figure, the effects of parameters can be investigated. Figure 16 shows the behavior of shear transfer forces acting on diagonal tension crack after shear failure.

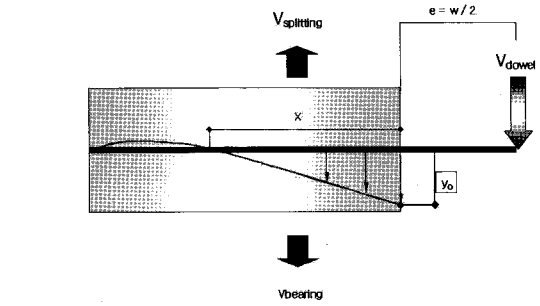

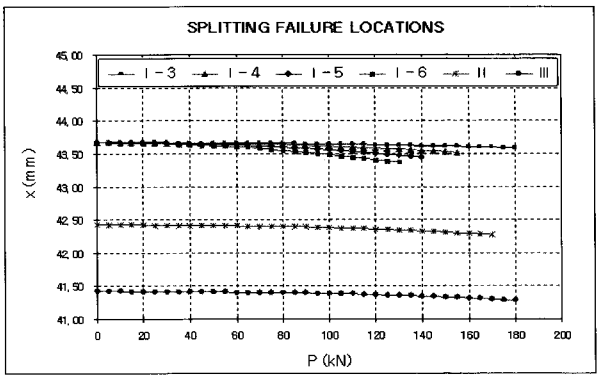

Fig. 13 Distance satisfying the equilibrium condition for splitting failure

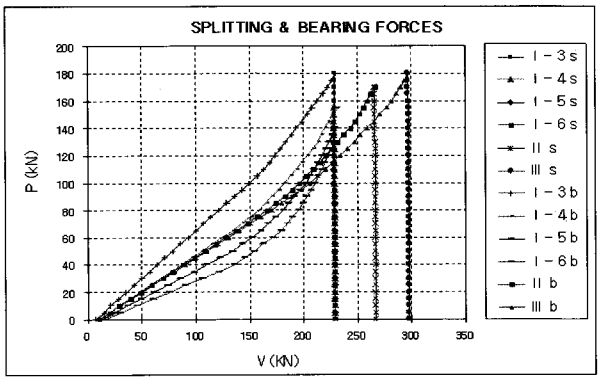

Fig. 14 Relations between bearing and splitting stresses

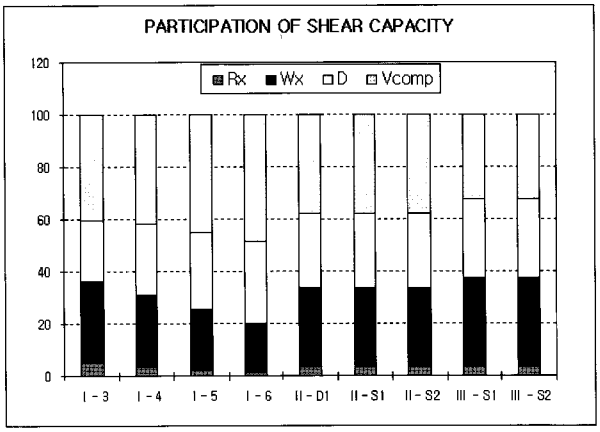

Fig. 15 Participating portions of shear transfer mechanisms

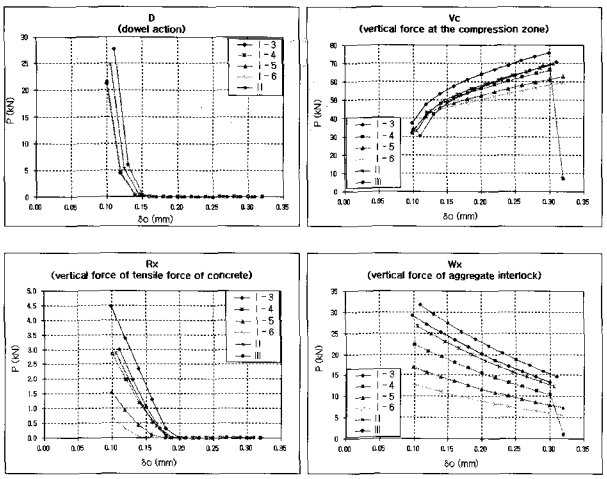

Fig. 16 Behavior of shear transfer forces after shear failure

4.5 Shear strength

Analytical results are compared with experimental formulas, which are ACI code, MC 90, and Remmel shown in Table 7. Table 8 shows the ratio between test results and others. According to this comparison, it is apparent that ACI code and MC 90 adopt the conservative formula for design purpose. Whereas Remmel's formula shows a good agreement with test results. The proposed model shows a good agreement with test results.

5. Conclusions

As a second part of this research, this paper verifies the efficiency of proposed model in part I. Comparing with test results, followings are concluded.

(1) Assumption about the location of critical shear crack initiation agrees well with test results for the shear slender beams. Whereas the shape of critical shear crack is somewhat different from test result, which show discordance even between the same beams. From the parameter study, ultimate shear strength is mainly influenced by the location of crack initiation, not crack shape.

(2) Assumed kinematical conditions, which are the rotation of shear crack and mean strain assumption of flexural crack zone, was reasonable according to the comparison between test and analytical results of mean strain values as well as crack width and sliding.

(3) Increasing shear span ratio decreases all the shear transfer forces besides dowel force due to increase of flexural capacity. Dowel force might be free in shear span ratio. Increasing concrete strength increases all shear transfer forces besides shear forces at the compression zone due to their direct relationship. Especially a proposal for aggregate interlock seems to be rational based on kinematical conditions or ultimate shear capacity. Decrease of shear force at the compression zone is due to increasing participation of other forces.

(4) Estimation of ultimate shear capacity by proposed model shows a good agreement with test results compared with representative calculated result by empirical formulas.

A detailed comparisons of analytical model with test results show that the proposed model can not explain whole aspects of shear behavior of shear slender beam. However, it contributes to the better estimation for each shear transfer mechanisms, tendency of behavior after ultimate load based on rational consideration of kinematical conditions.

Table 7 Comparison of crack opening and sliding between test and analysis

	Shear formula
ACI	$V_{cr} = (0.16\sqrt{f_c} + 17\rho\frac{Vd}{m})\cdot 10^3\, b\, d$
MC 90	$V_{cr} = 150\,(1+\sqrt{\frac{0.2}{d}})\,(\frac{3d}{a_s})^{1/3}\,(100\rho)^{1/3}\, f_c^{1/3}\, b\, d$
Remmel	$V_c = 1.4\cdot\sqrt{\frac{l_{ch}\cdot\rho}{d_s}}\cdot f_{ct}\cdot bd$

Table 8 Comparison of ultimate shear capacity

ID	V_{test}	$V_{proposal/test}$	$V_{ACI/test}$	$V_{MC90/test}$	$V_{Remmel/test}$
I - 3	70.6	1.31	0.86	0.93	1.01
I - 4	71.7	1.12	0.82	0.83	0.99
I - 5	75.7	0.96	0.77	0.73	0.94
I - 6	73.2	0.92	0.78	0.71	0.97
II - D1	92.1	0.95	0.75	0.73	0.90
II - S1	91.1	0.96	0.76	0.74	0.91
II - S2	84.4	1.04	0.82	0.79	0.98
III - S1	93.1	0.99	0.85	0.79	1.00
III - S2	87.4	1.06	0.91	0.84	1.07
Minimum		0.92	0.75	0.71	0.90
Maximum		1.31	0.91	0.93	1.07
Mean		1.03	0.81	0.79	0.97
Standard deviation		0.07	0.05	0.07	0.05

Acknowledgements

The research presented in this paper is supported by Korea Bridge Design and Engineering Research Center. This generous supports are greatly acknowledged.

References

Ahmad, A.R., Khaloo, A. and Poveda, A. (1986). "Shear Capacity of Reinforced High-Strength Concrete Beams", ACI-journal, Vol 83, No 2, pp 291-302.

Bahl, N.S. (1968). Über den Einfluß der Balkenhöhe auf die Schubtragfähigkeit von Einfeldrigen Stahlbetonbalken mit und Ohne Schubbevehrung, Schriftenreihe des Otto-Graf Institutes, Nr. 35, Stuttgart, Germany.

Leonhardt, F. and Walter, R. (1962), Schubversuche an einfeldrigen Stahlbetonbalken mit und ohne Schubbewehrung, DAfStb, H 151, Beuth, Berlin.

2007년 10월 26일 원고 접수
2007년 12월 24일 최종 수정본 채택